

Retrieval of cloud  
spherical albedo

A. Kokhanovsky et al.

# Retrieval of cloud spherical albedo from top-of-atmosphere reflectance measurements performed at a single observation angle

A. Kokhanovsky<sup>1</sup>, B. Mayer<sup>2</sup>, and W. von Hoyningen-Huene<sup>1</sup>

<sup>1</sup>Institute of Environmental Physics, University of Bremen, Otto Hahn Allee 1, 28334 Bremen, Germany

<sup>2</sup>Institute of Atmospheric Physics, Deutsches Zentrum für Luft- und Raumfahrt (DLR), Oberpfaffenhofen, 82234 Wessling, Germany

Received: 25 November 2005 – Accepted: 29 January 2006 – Published: 31 March 2006

Correspondence to: A. Kokhanovsky (alexk@iup.physik.uni-bremen.de)

Title Page

Abstract

Introduction

Conclusions

References

Tables

Figures

◀

▶

◀

▶

Back

Close

Full Screen / Esc

Printer-friendly Version

Interactive Discussion

EGU

## Abstract

The paper is devoted to the derivation of the simple analytical relationship between the cloud spherical albedo and the cloud reflection function. The relationship obtained can be used for the derivation of the spherical albedo from backscattered solar light measurements performed by radiometers on geostationary and polar orbiting satellites. The example of the application of the technique to MODIS data is shown.

## 1 Introduction

The spherical albedo  $r$  of a cloud is an important parameter for climate research (Twomey, 1974; Jacobowitz and Hucek, 1994). Therefore, it is of importance to derive the global cloud spherical albedo product from satellite observations (see, e.g., Diner et al., 2005). This is quite a difficult task because the value of  $r$  is an integral of the measured cloud reflection function with respect to angular variables (e.g., the solar and satellite observation angles, the relative azimuth). One way to derive the spherical albedo is to determine the cloud optical thickness and the effective droplet/ice crystal size from spectral top-of-atmosphere reflectance measurements (e.g., using a look-up-table technique). Subsequently, this information can be used for the calculation of  $r$ .

Interestingly, there is an alternative possibility of the direct determination of the spherical cloud albedo from single reflection function measurements for the special case of optically thick cloudiness. The proposed technique requires no a priori information on the size of droplets and the cloud optical thickness. The accuracy of the technique can be increased if information on the cloud thermodynamic state (e.g., from thermal infrared measurements) is known. The method proposed is based on the asymptotic radiative transfer equation solution valid for optically thick cloud layers (Kokhanovsky, 2005a; van de Hulst, 1980).

Title Page

Abstract

Introduction

Conclusions

References

Tables

Figures

◀

▶

◀

▶

Back

Close

Full Screen / Esc

Printer-friendly Version

Interactive Discussion

## 2 The determination of cloud spherical albedo

The reflection function  $R(\xi, \eta, \varphi)$  of an optically thick cloud can be presented in the following form in the visible (van de Hulst, 1980; Kokhanovsky, 2005a):

$$R(\xi, \eta, \varphi) = R_\infty(\xi, \eta, \varphi) - T(\xi, \eta), T(\xi, \eta) = tK(\xi)K(\eta), \quad (1)$$

where  $t$  is the diffuse cloud transmittance under diffuse illumination conditions,  $R_\infty(\xi, \eta, \varphi)$  is the reflection function of a semi-infinite cloud,  $T(\xi, \eta)$  is the cloud transmission function,  $K(\xi)$  is the escape function,  $\xi$  is the cosine of the solar angle,  $\eta$  is the cosine of the observation angle, and  $\varphi$  is the relative azimuth. This equation has a high accuracy for clouds with the optical thickness larger than 5 (Kokhanovsky, 2005a).

Taking into account that  $t=1-r$  due to the energy conservation law, we obtain from Eq. (1):

$$r = 1 - \frac{R_\infty(\xi, \eta, \varphi) - R(\xi, \eta, \varphi)}{K(\xi)K(\eta)} \quad (2)$$

This analytical result can be used to determine the cloud spherical albedo from the reflection function  $R(\xi, \eta, \varphi)$  measurements at a single viewing geometry. No additional information on cloud microphysical characteristics and cloud extent is needed for the retrieval procedure. However, the information on the cloud thermodynamic state is of importance. This is due to the fact that the function  $R_\infty(\xi, \eta, \varphi)$  actually depends on the shape of scatterers. The dependence of  $R_\infty(\xi, \eta, \varphi)$  on the size of particles can be neglected as demonstrated by Kokhanovsky et al. (2003). This means that the pre-calculated look-up-table of  $R_\infty(\xi, \eta, \varphi)$  can be used in combination with Eq. (2) for the direct determination of the water cloud spherical albedo from satellite observations. Yet another look-up-table must be constructed for the specific case of ice clouds.

The escape function  $K(\xi)$  in Eq. (2) is insensitive to the shape/size of scatterers (Kokhanovsky, 2003) and can be approximated as follows:

$$K(\xi) = \frac{3}{7}(1 + 2\xi) \quad (3)$$

### Retrieval of cloud spherical albedo

A. Kokhanovsky et al.

Title Page

Abstract

Introduction

Conclusions

References

Tables

Figures

◀

▶

◀

▶

Back

Close

Full Screen / Esc

Printer-friendly Version

Interactive Discussion

## Retrieval of cloud spherical albedo

A. Kokhanovsky et al.

Title Page

Abstract

Introduction

Conclusions

References

Tables

Figures

◀

▶

◀

▶

Back

Close

Full Screen / Esc

Printer-friendly Version

Interactive Discussion

EGU

This is due to the fact that this function describes the angular distribution of photons escaping from a semi-infinite nonabsorbing media with sources located deep inside the medium. Therefore, multiple light scattering washes out almost all features characteristic for a single scattering law (at least for  $\xi \geq 0.2$ , which is a standard case for most cloud remote sensing problems). To check the theoretical result as shown in Eq. (3), we have performed measurements of the angular distribution of light transmitted by a cloud in the principal plane using Automatic Sun Tracking Photometer CE318. The details of the instrument are given at <http://www.cimel.fr>.

The cloud was composed of precipitating ice crystals. Results of measurements are given in Fig. 1. Indeed, we see that measurements nicely follow the cosine law as predicted by Eq. (3). The broken line corresponds to the value of the escape function given by Eq. (3) divided by  $K(1)=9/7$ .

Substituting Eq. (3) in Eq. (2), we get:

$$r = 1 - \frac{49(R_\infty(\xi, \eta, \varphi) - R(\xi, \eta, \varphi))}{9(1 + 2\xi)(1 + 2\eta)}, \quad (4)$$

where  $R(\xi, \eta, \varphi)$  must be obtained from measurements and  $R_\infty(\xi, \eta, \varphi)$  is given either in a correspondent look-up-table or by an approximation (Kokhanovsky, 2005a). In particular, the following approximation for  $R_\infty(\xi, \eta, \varphi)$  in the case of water clouds can be used (Kokhanovsky, 2005a):

$$R_\infty(\xi, \eta, \varphi) = \frac{0.37 + 1.94\xi}{1 + \xi} + \frac{\rho(\pi - \cos^{-1} \xi)}{4(1 + \xi)} \quad (5)$$

at the nadir observation conditions. Here,  $\rho(\pi - \cos^{-1} \xi)$  is the cloud phase function.

The accuracy of Eq. (4) is shown in Fig. 2a. The spherical albedo for solar zenith angles 0, 30, 45, and 60° was obtained using the numerical solution of the radiative transfer equation in the framework of libradtran package (Kylling and Mayer, 2005) for different cloud optical thickness  $\tau$  in the range 1–5000 (solid line in Fig. 2a). Calculations were performed at the wavelength 650 nm for the gamma droplet size distribution

## Retrieval of cloud spherical albedo

A. Kokhanovsky et al.

Title Page

Abstract

Introduction

Conclusions

References

Tables

Figures

◀

▶

◀

▶

Back

Close

Full Screen / Esc

Printer-friendly Version

Interactive Discussion

with the effective radius  $6\ \mu\text{m}$  and the coefficient of variance equal to 0.37. Effects of light absorption were neglected. Broken lines give calculations of  $r$  using Eq. (4) with  $R_\infty(\xi, \eta, \varphi)$  and  $R(\xi, \eta, \varphi)$  obtained from libradtran. It follows that there is dependence of  $r$  on the solar zenith angle at  $\tau \leq 10$ . This means that Eq. (2) is not suitable for the case of thin clouds. However, for thicker clouds solid and broken lines coincide. This confirms the applicability of the technique for optically thick clouds. The absolute value of the error is smaller than 10% at  $\tau \geq 6$ . The error is below 3% at  $\tau \geq 10$  for all considered solar zenith angles and nadir observations (see Fig. 2b). It follows from Fig. 3 that the method can be recommended for the values of the spherical albedo larger than 0.5 (or even 0.4, depending on the accuracy required).

Figure 4 shows the performance of Eq. (4) when  $R_\infty(\xi, \eta, \varphi)$  is calculated using Eq. (5). In this calculation, we neglect a priori unknown second term in Eq. (5). It follows that the absolute error is below 5% at  $\tau \geq 10$  for all angles except the case of the solar zenith angle  $0^\circ$ , where one must account for the phase function in Eq. (5). This allows for the correct consideration of glory scattering.

We find that the following analytical result can be used for the spherical albedo determination from measurements of  $R(\xi, \eta, \varphi)$ :

$$r = 1 - \frac{2 + 10.56\xi - 5.44(1 + \xi)R(\xi, \eta, \varphi)}{(1 + \xi)(1 + 2\xi)(1 + 2\eta)}. \quad (6)$$

This formula is derived combining Eqs. (4), (5) (at  $p=0$ ).

### 3 The application of the technique to satellite data

We applied the technique described above for studies of cloud spherical albedo of Hurricane Katrina using top-of-atmosphere reflectance measurements of MODIS on Terra satellite. Hurricane Katrina has originated as a Tropical Depression on 23 August 2005 at (23.2° N, 75.5° W). Hurricane has propagated initially to north-west, then to west and finally to north and then to north-east (after landfall in New Orleans). The

**Retrieval of cloud spherical albedo**

A. Kokhanovsky et al.

[Title Page](#)[Abstract](#)[Introduction](#)[Conclusions](#)[References](#)[Tables](#)[Figures](#)[I◀](#)[▶I](#)[◀](#)[▶](#)[Back](#)[Close](#)[Full Screen / Esc](#)[Printer-friendly Version](#)[Interactive Discussion](#)

retrieved spherical albedo map for 28 August 2005 (17:00 UTC) is shown in Fig. 5. MODIS data at 645 nm with the spatial resolution 1 km was used for the creation of this map. Therefore, the spatial scale on the map shown in Fig. 5 corresponds to 1 km. The cloud spherical albedo retrieval is based on Eq. (2) with  $R_{\infty}(\xi, \eta, \varphi)$  found for a special case of crystalline clouds as described by Kokhanovsky (2005b). This is due to the fact that tops of hurricanes are covered by ice clouds.

We see that Katrina occupies the huge area of approximately  $400 \times 800 \text{ km}^2$ . At this date Katrina was classified as Hurricane category 5 with winds 175 mph and a minimum pressure of 902 mbar. The next day Katrina was downgraded to Category 4 hurricane and made a landfall in New Orleans devastating the area.

It follows that hurricane is characterized by quite large values of spherical albedo (larger than 0.9 for the central part of a hurricane). The spherical albedo in an eye is somewhat smaller (around 0.7–0.8). It means that an eye is occupied by quite thick clouds. The histogram of cloud spherical albedo is shown in Fig. 6. Colors in Figs. 5 and 6 have the same meaning. So we conclude that the spherical albedo of a hurricane is larger than 0.6 for most of  $1 \times 1 \text{ km}^2$  pixels studied. Blue color corresponds to relatively thin clouds on the periphery of the cloud system. Here broken cloud conditions can influence retrievals considerably.

#### 4 Conclusion

We propose here a simple analytical equation, which can be used for the determination of cloud spherical albedo from top-of-atmosphere reflectance measurements (at a single viewing geometry). This procedure does not require a priori knowledge of the cloud optical thickness and the effective radius of scatterers. The spherical albedo map and also the frequency of occurrence of  $r$  for Hurricane Katrina were studied. It was found that the most frequent value of spherical albedo is around 0.9 for Category 5 Hurricane Katrina with the largest fraction of clouds with albedos in the range 0.6–0.95. This finding confirms that hurricanes are strong reflectors of visible radiation back to space.

This could have important climatic effects taking into account the increased frequency of strong hurricanes in recent years.

## References

- 5 Diner, D. J., Braswell, B. H., Davies, R., Gobron, N., Hu, J., Jin, Y., Kahn, R. A., Knyazikhin, Y., Loeb, N., Muller, J.-P., Nolin, A. W., Pinty, B., Schaaf, C. B., Seiz, G., and Stroeve, J.: The value of multiangle measurements for retrieving structurally and radiatively consistent properties of clouds, aerosols, and surfaces, *Rem. Sens. Environ.*, 97, 495–518, 2005.
- Jacobowitz, H. and Hucek, R.: Improvements in broadband planetary albedo estimates from narrowband NOAA satellite observations, *Adv. Space Res.*, 14, 99–102, 1994.
- 10 Kokhanovsky, A. A., Rozanov, V. V., Zege, E. P., Bovensmann, H., and Burrows, J. P.: A semianalytical cloud retrieval algorithm using backscattered radiation in 0.4–2.4  $\mu\text{m}$  spectral band, *J. Geophys. Res.*, 108, doi:10.1029/2001JD001543, 2003.
- Kokhanovsky, A. A.: *Cloud optics*, Berlin, Springer, 2005a.
- Kokhanovsky, A. A.: Reflection of light from particulate media with irregularly shaped particles, *J. Quant. Spectr. Rad. Transfer*, 96, 1–10, 2005b.
- 15 Kylling, A. and Mayer, B.: Technical note: The libRadtransoftware package for radiative transfer calculations – description and examples of use, *Atmos. Chem. Phys.*, 5, 1855–1877, 2005.
- Twomey, S.: Pollution and planetary albedo, *Atmos. Environ.*, 8, 1251–1256, 1974.
- Van de Hulst, H. C.: *Multiple light scattering*, N.Y., Academic Press, 1980.

## Retrieval of cloud spherical albedo

A. Kokhanovsky et al.

Title Page

Abstract

Introduction

Conclusions

References

Tables

Figures

◀

▶

◀

▶

Back

Close

Full Screen / Esc

Printer-friendly Version

Interactive Discussion

Retrieval of cloud  
spherical albedo

A. Kokhanovsky et al.

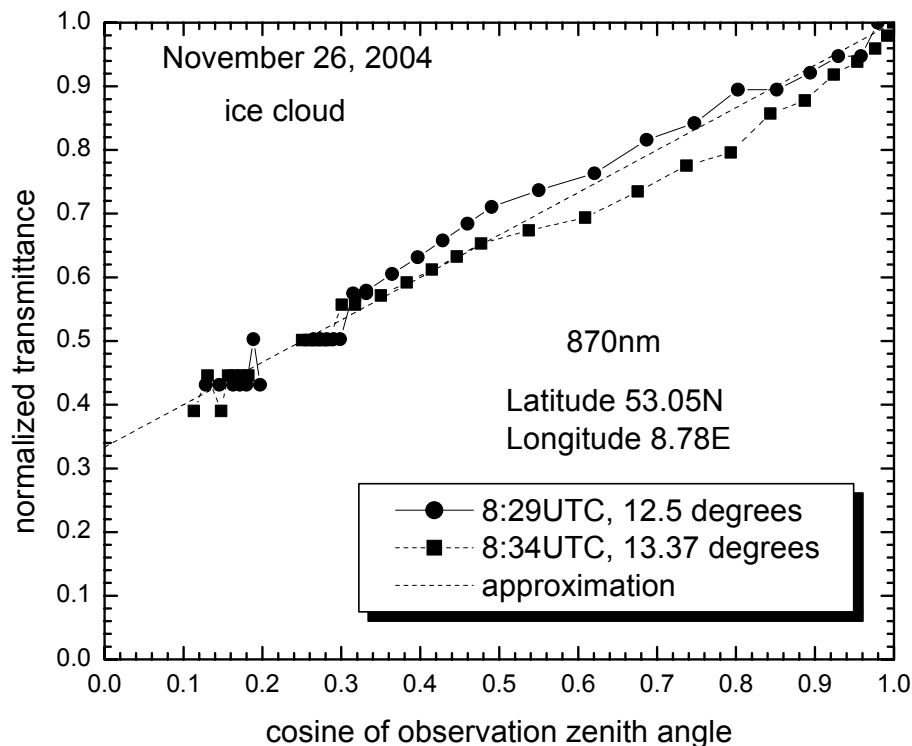


**Fig. 1.** The cloud transmittance divided by its value at the zenith. Measurements have been performed under crystalline optically thick precipitating cloud conditions in Bremen (northern Germany) on 24 November 2004. Only results for the principal plane measurements at the wavelength 870 nm are shown. Solar zenith angles were 12.5 (08:29 UTC) and 13.37 (08:34 UTC) degrees, respectively. The field of view was 1.2°.

[Title Page](#)[Abstract](#)[Introduction](#)[Conclusions](#)[References](#)[Tables](#)[Figures](#)[◀](#)[▶](#)[◀](#)[▶](#)[Back](#)[Close](#)[Full Screen / Esc](#)[Printer-friendly Version](#)[Interactive Discussion](#)

EGU



## Retrieval of cloud spherical albedo

A. Kokhanovsky et al.

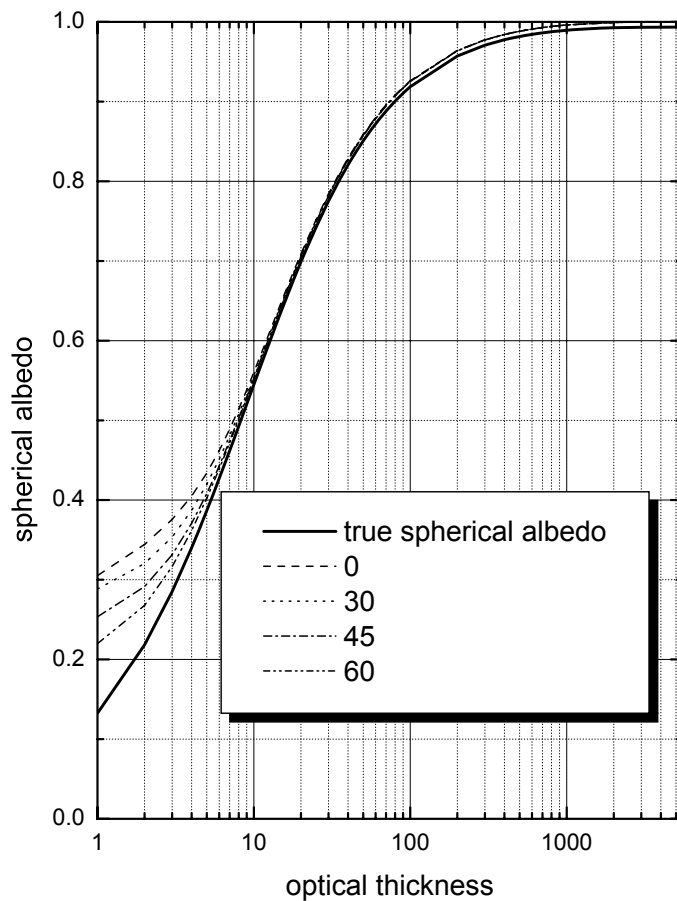


**Fig. 2a.** Spherical albedo calculated using exact radiative transfer code (solid line) and also obtained using approximate Eq. (1) for several solar incidence angles (0, 30, 45, and 60°) as function of cloud optical thickness.

[Title Page](#)[Abstract](#)[Introduction](#)[Conclusions](#)[References](#)[Tables](#)[Figures](#)[◀](#)[▶](#)[◀](#)[▶](#)[Back](#)[Close](#)[Full Screen / Esc](#)[Printer-friendly Version](#)[Interactive Discussion](#)

**Retrieval of cloud spherical albedo**

A. Kokhanovsky et al.

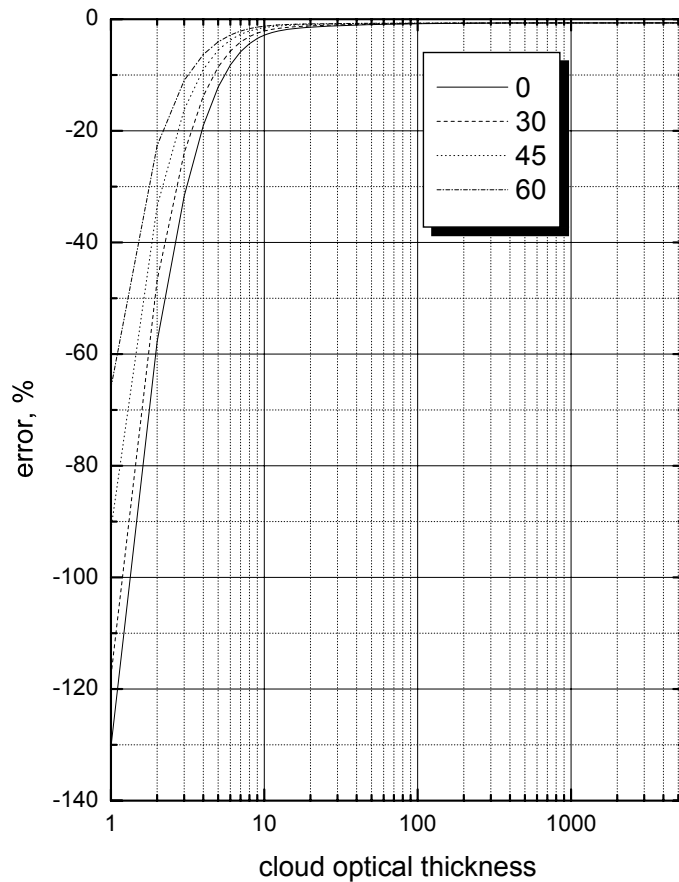


**Fig. 2b.** Error of Eq. (1) at several observation angles as function of cloud optical thickness.

[Title Page](#)[Abstract](#)[Introduction](#)[Conclusions](#)[References](#)[Tables](#)[Figures](#)[◀](#)[▶](#)[◀](#)[▶](#)[Back](#)[Close](#)[Full Screen / Esc](#)[Printer-friendly Version](#)[Interactive Discussion](#)

**Retrieval of cloud  
spherical albedo**

A. Kokhanovsky et al.

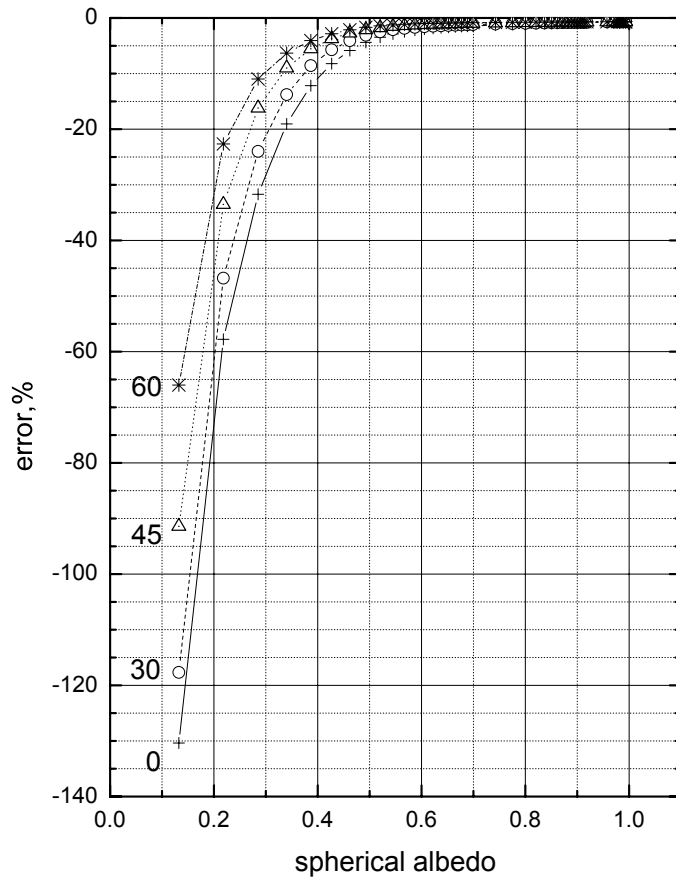


**Fig. 3.** The same as in Fig. 2b except as the function of cloud spherical albedo.

[Title Page](#)[Abstract](#)[Introduction](#)[Conclusions](#)[References](#)[Tables](#)[Figures](#)[◀](#)[▶](#)[◀](#)[▶](#)[Back](#)[Close](#)[Full Screen / Esc](#)[Printer-friendly Version](#)[Interactive Discussion](#)

Retrieval of cloud  
spherical albedo

A. Kokhanovsky et al.

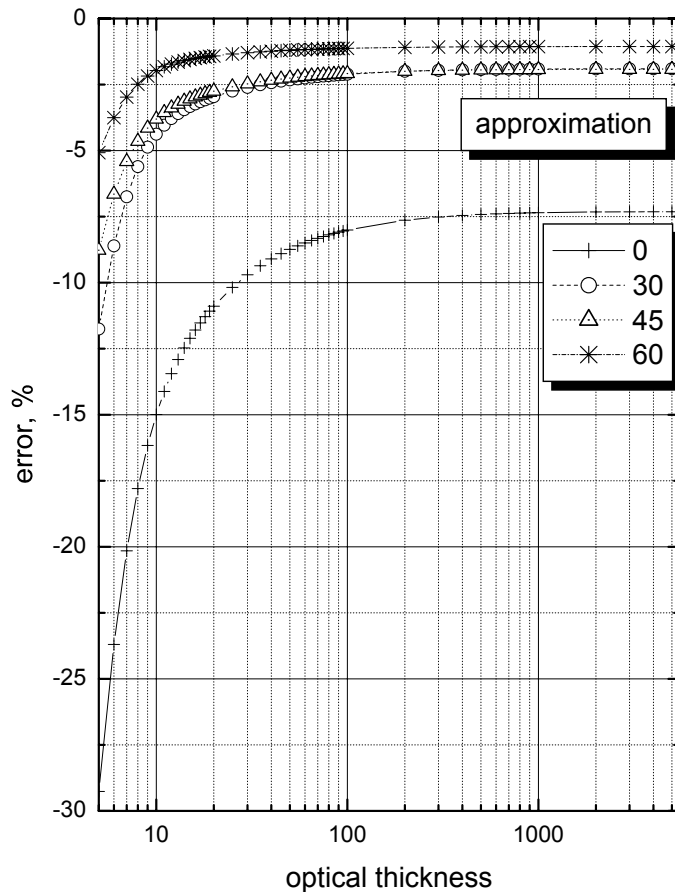


**Fig. 4.** The same as in Fig. 2b except reflection function of semi-infinite cloud in Eq. (1) is calculated using Eq. (3) assuming  $p=0$ .

[Title Page](#)[Abstract](#)[Introduction](#)[Conclusions](#)[References](#)[Tables](#)[Figures](#)[◀](#)[▶](#)[◀](#)[▶](#)[Back](#)[Close](#)[Full Screen / Esc](#)[Printer-friendly Version](#)[Interactive Discussion](#)

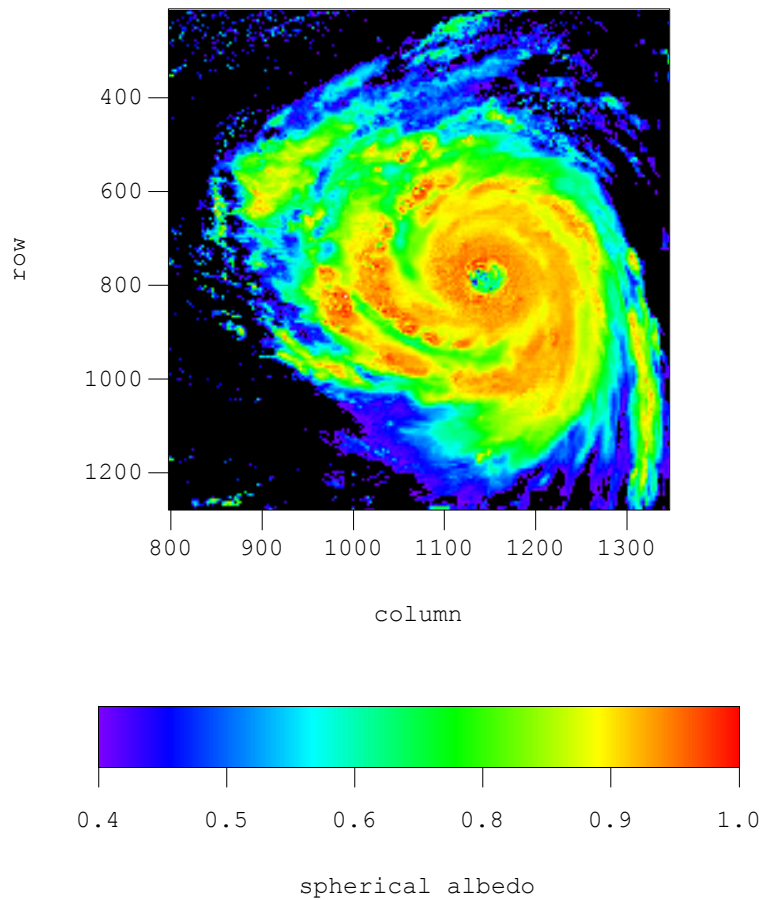


**Fig. 5.** The spherical albedo map.

**Retrieval of cloud spherical albedo**

A. Kokhanovsky et al.

Title Page

Abstract

Introduction

Conclusions

References

Tables

Figures

◀

▶

◀

▶

Back

Close

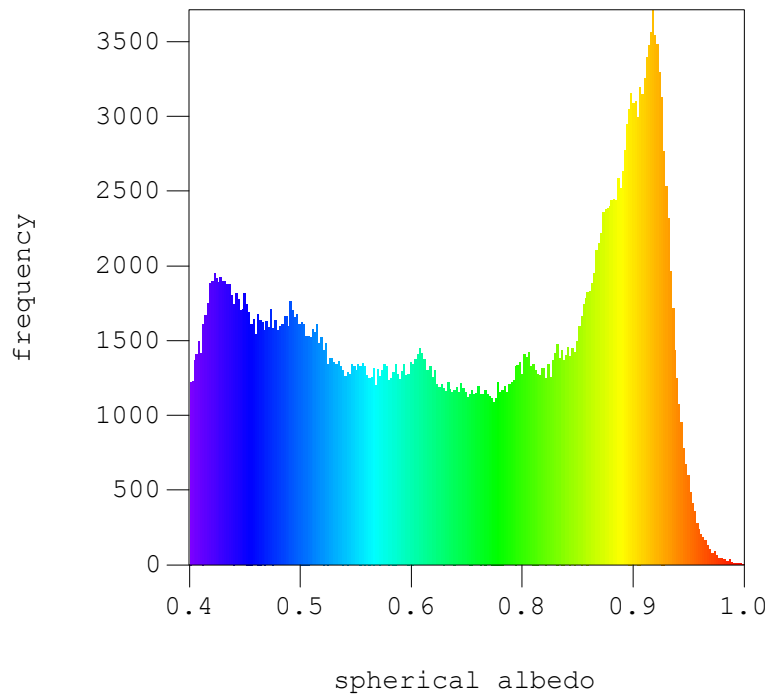
Full Screen / Esc

Printer-friendly Version

Interactive Discussion

**Retrieval of cloud  
spherical albedo**

A. Kokhanovsky et al.

**Fig. 6.** The spherical albedo histogram.[Title Page](#)[Abstract](#)[Introduction](#)[Conclusions](#)[References](#)[Tables](#)[Figures](#)[◀](#)[▶](#)[◀](#)[▶](#)[Back](#)[Close](#)[Full Screen / Esc](#)[Printer-friendly Version](#)[Interactive Discussion](#)